

Loss of Bloom syndrome protein destabilizes human gene cluster architecture

Michael W. Killen¹, Dawn M. Stults², Noritaka Adachi³, Les Hanakahi⁴ and Andrew J. Pierce^{1,2,*}

¹Department of Microbiology, Immunology and Molecular Genetics and ²Department of Toxicology, Markey Cancer Center, University of Kentucky, Lexington, KY, USA, ³Department of Genome System Science, Graduate School of Nanobioscience, Yokohama City University, Yokohama, Japan, ⁴Department of Biochemistry and Molecular Biology, Bloomberg School of Public Health, Johns Hopkins University, Baltimore, MD, USA

Received May 12, 2009; Revised and Accepted June 15, 2009

Bloom syndrome confers strong predisposition to malignancy in multiple tissue types. The Bloom syndrome patient (BLM) protein defective in the disease biochemically functions as a Holliday junction dissolvase and human cells lacking functional BLM show 10-fold elevated rates of sister chromatid exchange. Collectively, these phenomena suggest that dysregulated mitotic recombination drives the genomic instability underpinning the development of cancer in these individuals. Here we use physical analysis of the highly repeated, highly self-similar human ribosomal RNA gene clusters as sentinel biomarkers for dysregulated homologous recombination to demonstrate that loss of BLM protein function causes a striking increase in spontaneous molecular level genomic restructuring. Analysis of single-cell derived sub-clonal populations from wild-type human cell lines shows that gene cluster architecture is ordinarily very faithfully preserved under mitosis, but is so unstable in cell lines derived from BLMs as to make gene cluster architecture in different sub-clonal populations essentially unrecognizable one from another. Human cells defective in a different RecQ helicase, the WRN protein involved in the premature aging Werner syndrome, do not exhibit the gene cluster instability (GCI) phenotype, indicating that the BLM protein specifically, rather than RecQ helicases generally, holds back this recombination-mediated genomic instability. An ataxia-telangiectasia defective cell line also shows elevated rDNA GCI, although not to the extent of BLM defective cells. Genomic restructuring mediated by dysregulated recombination between the abundant low-copy repeats in the human genome may prove to be an important additional mechanism of genomic instability driving the initiation and progression of human cancer.

INTRODUCTION

Early onset of multiple malignancies is a clinical hallmark of Bloom syndrome, with mean age of death in Bloom syndrome patients (BLMs) younger than 24 years (1) suggesting a critical loss of genomic stability. Cytologically, cells from BLMs show a 10-fold elevation in rates of sister chromatid exchange (SCE) when differentially stained following incorporation of various thymidine analogs, as well as a spontaneous increase in chromosomal abnormalities such as quadriradial structures (2,3). Although dramatic in appearance when visualized in the standard assay for SCE (4), exchanges between sister chromatids are genetically silent, and therefore not directly contributory

to genomic instability *per se*. Nevertheless, the class of genomic alteration represented by SCE, the physical relocation of genetic material, without associated change in either the amount or sequence of this material, is an important but poorly examined mechanism of chromosomal alteration, particularly when these alterations are in the sub-microscopic size range. In this report, we present a sensitive assay of ribosomal gene cluster instability (GCI) that demonstrates exactly this kind of non-silent molecular level alterations to chromosomal architecture resulting from the absence of the Bloom syndrome protein. We also use this assay to show that unlike loss of the Bloom syndrome protein, neither loss of the BLM-related Werner protein nor inactivation of either transcription-coupled

*To whom correspondence should be addressed at: 207 Combs Research Building, 800 Rose Street, Lexington, KY 40536-0096, USA. Tel: +1 8593231455; Fax: +1 8592578940; Email: andrew.pierce@uky.edu

nucleotide excision repair or non-homologous end-joining (NHEJ) appreciably increase this GCI.

The BLM protein inactivated in BLMs is a member of the RecQ helicase family of helicases (5). In humans, there are five known RecQ homologs implicated in the maintenance of genomic stability (reviewed in 6). Mechanistically, the BLM protein, in conjunction with binding partners RMI1, RMI2 and TOP3A (7,8), can function as a Holliday junction dissolvase (9,10) that reverses the strand exchanges in a double Holliday junction structure to prevent potential junction resolution involving crossover products. In the absence of sufficient BLM-complex activity, such recombination intermediates may be subject instead to resolution by the human Holliday junction resolvase GEN1 (11), with the risk of production of both crossover and non-crossover products.

Although crossover recombination between precisely aligned sister chromatids is not inherently destabilizing, the human genome contains abundant low-copy repeats (LCRs) with sufficiently high levels of sequence similarity as to be susceptible to non-allelic homologous recombination (NAHR) (12). Structural alterations to genomic architecture caused by NAHR between LCRs include deletions, inversions and translocations with the possible generation of both acentric and dicentric chromosomes (reviewed in 13). Although the consequences of recombination-mediated genomic restructuring can be dire, spontaneous occurrences of NAHR are rare, hindering the identification of genetic components important for suppressing this class of genomic instability. Early work with BLM defective cells gave phenotypic evidence that the BLM protein could suppress NAHR in repetitive genomic loci (14,15), later supported by molecular evidence of loss of heterozygosity between parentally homologous chromosomes (16,17), and in instability of a 40 bp repetitive mini-satellite sequence (18). We now extend this work to much larger gene clusters distributed on multiple chromosomes.

Large gene clusters possess attributes predicted to be conducive to recombinational alteration. The repeated genes that make up clusters tend to have very high levels of sequence identity, sufficient length to be substrates for recombination, and occur in high local concentration with respect to each other. The gene clusters encoding the 45S precursor transcript to the 18S, 5.8S and 28S ribosomal RNA molecules (collectively the 'rDNA') are perhaps the largest clustered gene arrangement in the human genome, with approximately 600 repeats of the unit 43 kb gene (19) divided among the five pairs of acrocentric chromosomes (20). We recently characterized the physical lengths of these rDNA gene clusters in human individuals and found essentially complete cluster length heterozygosity, both between clusters on different acrocentric chromosomes and also between clusters on individual parental homolog chromosome pairs (21). This cluster length heterogeneity is driven by strong meiotic recombination at a rate of over 10% per cluster per meiosis. We were also able to detect spontaneous mitotic rearrangement in these clusters, suggesting that they would be suitable as sentinel biomarkers for dysregulated recombination. Accordingly, we screened a panel of cell lines representing diverse human chromosomal instability syndromes for hyper-recombination in the rDNA gene clusters and used both shRNA knockdowns and complemented mutant cell

lines to establish that the BLM protein is a crucial suppressor of GCI.

RESULTS

We assay dysregulated recombination by ascertaining the stability of the length of gene clusters. The lengths are determined by restriction digestion of high molecular weight genomic DNA with enzymes that do not have a recognition site in the repeated gene unit. Since the repeated genes in clusters are generally highly conserved, an enzyme that does not cut in one repeat tends not to cut in any and can thereby liberate intact gene clusters from bulk genomic DNA, with the addition of a small amount of randomly sized flanking DNA (Fig. 1A). Liberated gene clusters can then be separated by size using pulsed-field gel electrophoresis and identified by Southern blotting. The goal is to utilize this pulsed-field based assay to quantify the GCI in human cells. In any cell population derived from a single cell, including human individuals, genomic gene clusters will have a well-defined initial length. We call the size-resolved pattern of these initial cluster lengths the 'major banding pattern' (Fig. 1B, 'Initial Pattern'). As the cell population expands, if the gene clusters are completely stable, the initial cluster lengths found in the progenitor cell will be faithfully transmitted to all subsequent daughter cells (Fig. 1B, 'No GCI'). Alternatively, recombination in the expanding population can generate sub-populations with altered gene cluster lengths. Since these sub-populations only represent a fraction of the total population, bands detected by Southern blotting will be reduced in intensity accordingly. We call these reduced-intensity bands the 'minor banding population' (Fig. 1B, 'Low GCI'). The amount of this minor-intensity banding found in any cell population is indicative of the degree of GCI in that population. Since recombination requires precise alignment of homologous sequences, cluster lengths can only change by integer multiples of the unit repeat length. This constraint upon allowable gene cluster lengths (Fig. 1B, dotted lines) means that very high levels of instability will generate a ladder-like pattern of bands in a Southern blot (Fig. 1B, 'High GCI'), consistent with a recombination-based mechanism. If cluster length alterations were due to random breakage and rejoining, a smear would be observed, rather than a ladder.

We screened a panel of cell lines including various known human chromosomal instability syndromes (Fig. 1C). Stable gene clusters result in a well-defined pattern of major bands, with largely empty intervening space and few minor bands. As expected, since every individual human has a unique pattern of major bands (21), the human cell lines also possess unique patterns of major bands. Instability will be indicated by the presence of minor-intensity bands. Four lines wild-type for major DNA repair pathways, BJ-5ta, CGM1, GM06990 and HeLa S3 (left side of the panel), largely exhibit such gene cluster stability, with only a few minor-intensity bands observed. BJ-5ta is immortalized by the expression of telomerase, CGM1 and GM06990 by EBV and HeLa S3 is a cultured cancer line, collectively indicating that cellular transformation and immortalization *per se* is

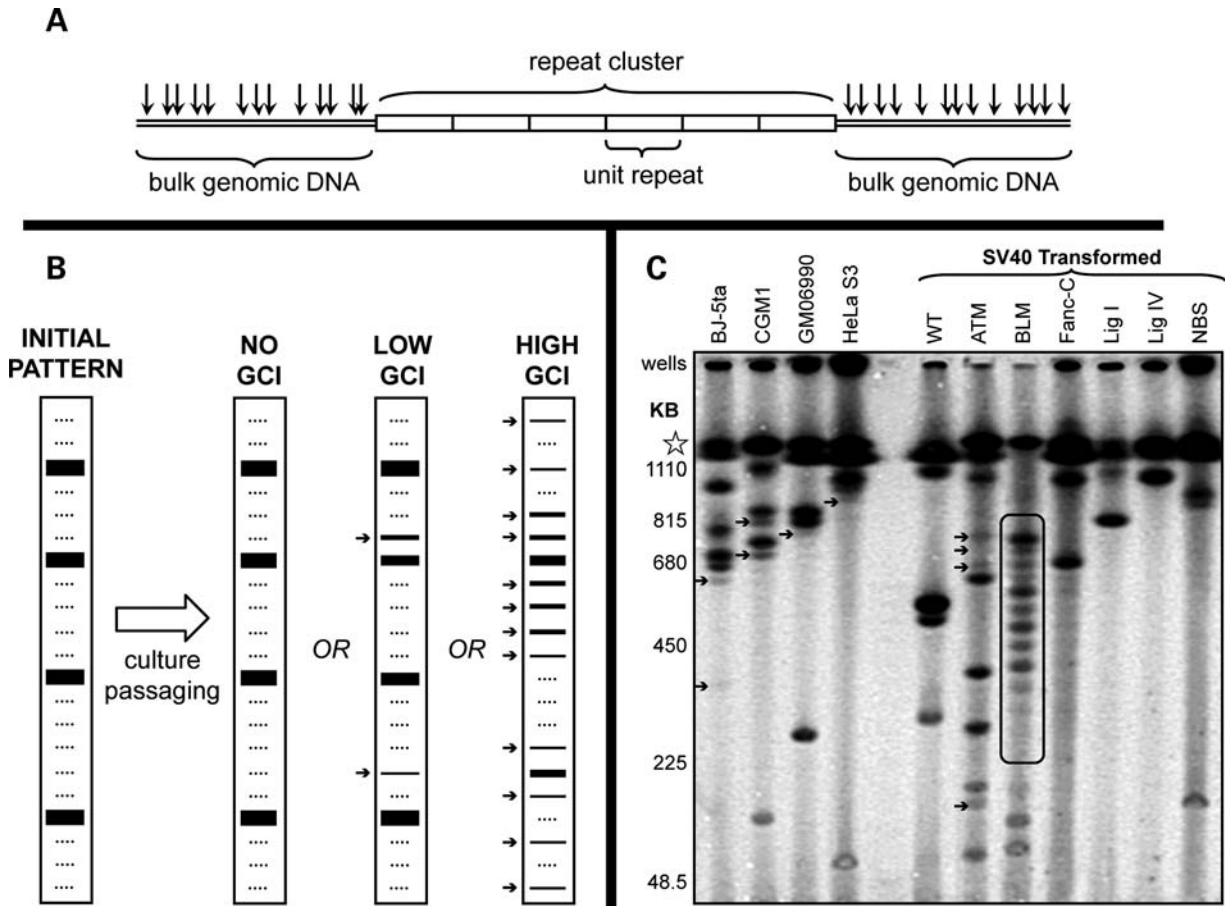


Figure 1. Screening cell lines for gene cluster instability (GCI) (A) Experimental strategy. Digestion of genomic DNA with restriction enzymes that do not cut within an individual gene cluster repeat liberates intact gene clusters from bulk genomic DNA. Panel from Stults *et al.* (21) (used with permission). (B) Schematic of GCI patterns in clonal cell lines. A single cell shows a well-defined pattern of gene cluster lengths ('Initial Pattern'—thick bands). Allowable, but currently unrepresented gene cluster lengths are shown as dotted lines. As mitotic division expands the clonal cell population in the absence of instability, gene cluster lengths are faithfully preserved ('No GCI'). Alternatively, instability generates sub-populations within the expanding population with altered cluster lengths giving rise to lower intensity 'minor bands' ('Low GCI'—thin bands indicated by arrows). High levels of instability generate a ladder-like pattern of minor banding with individual bands on the ladder differing by integer multiples of the unit repeat length ('High GCI'). (C) Screening non-clonal cell populations. Cluster lengths are resolved up to 1 Mb in length, with sizes shown from yeast chromosome markers. Unresolved clusters larger than 1 Mb run together at the gel resolution limit (star). Cell lines indicated at the top. Minor bands indicated by arrows. The ladder-like banding pattern indicative of high GCI is seen in the gene clusters from the BLM deficient cells (rounded box). BJ-5ta: wild-type newborn foreskin fibroblasts immortalized by ectopic telomerase expression; CGM1, GM06990: EBV-transformed wild-type lymphoblast lines; HeLa S3: cervical carcinoma cells; SV40-transformed fibroblast lines: WT: wild-type (GM00637); ATM: ataxia-telangiectasia mutated (GM09607); BLM: Bloom syndrome (GM08585); Fanc-C: Fanconi anemia complementation group C mutated (GM13136); Lig I: DNA ligase 1 defective (GM16097); Lig IV: DNA ligase IV defective (GM16089); NBS: Nijmegen breakage syndrome (GM15989).

generally not destabilizing to the faithful transmission of gene cluster lengths. Of the SV40-transformed lines from a panel of patients exhibiting defects in a variety of DNA repair pathways (right side of the panel), only that derived from a BLM is strongly destabilized (rounded box), with a clear ladder-pattern consistent with integer multiple differences of 43 kb: the size of the repeated rRNA genes. In contrast, the wild-type, DNA ligase 1-defective, DNA ligase IV-defective and Nijmegen breakage syndrome lines appear to be gene cluster stable. The ATM cells show minor banding consistent with a GCI-low phenotype; the HeLa and ATM cells are explored in more detail in Figure 7.

The basic GCI screen (Fig. 1) measures the amount of GCI that has occurred in the history of a given cell population rather than the rate at which GCI occurs. In this context, we

can understand the presence of minor bands in the GCI profile of a cell population as being the result of a gradual cumulative stochastic process of recombination-mediated alterations from the initial major banding pattern subjected to genetic drift. The fraction of cells in a cultured population that has gene cluster lengths not represented in the major banding pattern is a function of the inherent GCI rate of the cells in question, the total number of cell divisions undergone by the culture, and the degree to which the culture has been subjected to population bottlenecks.

We can uncover the GCI rate by unrestricted expansion of single-cell derived sub-clones. This procedure, in essence Luria–Delbruck fluctuation analysis (22), is sensitive only to the GCI rate since freely expanded sub-clonal populations experience the same number of cell divisions and no population

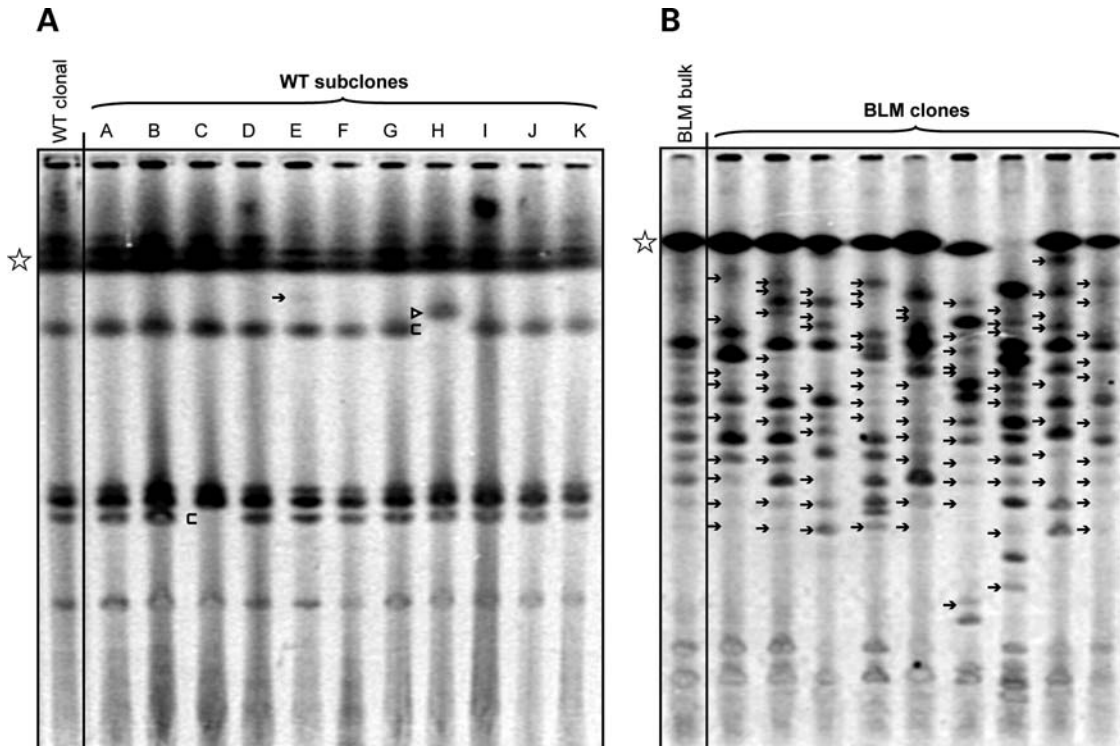


Figure 2. GCI clonal analysis. (A) Wild-type SV40-transformed GM00637 fibroblast cells. The gel resolves gene clusters up to 1 Mb in length (star). A clonal population derived from a single cell is shown in the leftmost lane. Sub-clones were derived by dilution plating to single cells with subsequent expansion. Minor bands indicated by arrows. Changes to the major banding pattern shown by triangles (new bands) and brackets (missing bands). (B) SV40-transformed fibroblast GM08505 Bloom syndrome cells. The bulk population as received from Coriell is shown in the far left. Clonal populations derived from the expansion of plated single cells from this bulk population are shown in the right. Minor bands indicated by arrows.

bottlenecks. Sub-cloning cell populations from single cells can be applied iteratively: minor bands in any parental population will produce new major bands in derivative sub-clonal populations with a frequency of occurrence determined by the fractional intensity of the minor bands in the parental population. New spontaneous GCI in any sub-clonal population will appear as *de novo* minor bands. This clonal GCI analysis of the wild-type GM00637 cell line (Fig. 2A) shows relatively stable gene cluster lengths. The lane 'WT clonal' is derived from a single cell. Single-cell derived sub-clones from this clonal population are shown in the right of the panel. Changes to the major banding pattern in the sub-clones are seen in sub-clones 'C' and 'H' (triangle and brackets indicating new major band and missing major bands, respectively). These represent mitotic gene cluster alterations occurring in the expansion of the 'WT clonal' cells that occurred too late in the expansion to yield visible minor bands in the 'WT clonal' lane. A minor band (arrow) is seen in sub-clone 'E', from a spontaneous gene cluster length alteration in the expansion of this individual sub-clone. We can reliably detect minor bands with an intensity of $\sim 10\%$ of the major bands. For 10% of the population to show an altered gene cluster length, the alteration had to occur sometime in the initial three or four rounds of cell division, i.e. before the population derived from a single cell had expanded to a total of 10 cells. In contrast to the rare minor banding of the wild-type population, the Bloom syndrome line GM08505 (Fig. 2B) shows such extensive minor banding that for practical purposes no major

banding pattern of rDNA gene clusters can be defined. Gene cluster lengths in the BLM cells are changing on the order of every mitotic division.

To establish that the genetic defect causing the GCI-high phenotype in the BLM-syndrome GM08505 cells is lack of BLM, we surveyed BLM lines derived from three other individual BLMs (Fig. 3A and B). The bulk wild-type cell populations appear stable with well-defined major bands and little or no minor banding evident. In contrast, each of the three BLM-patient derived lines, BLM Ash.1, BLM Ash.2 and BLM F.C., shows the ladder-pattern indicative of the GCI-high phenotype. BLM Ash.1 and BLM Ash.2 are from patients of Ashkenazi Jewish descent, each homozygous for the 6 bp deletion/7 bp insertion frameshifting Ashkenazi founder mutation. BLM F.C. is from a French-Canadian Bloom patient and is homozygous for a S595X translation terminating mutation. All three lines show a distinct ladder-pattern of minor bands (rounded boxes).

In order to determine whether the gene cluster destabilization preceded either transformation or tumorigenesis, we analyzed cells from primary fibroblast explants (Fig. 3B). Primary cells from an apparently healthy 11-year-old girl (GM10652) show well-defined major bands, and no minor banding, whereas primary cells from a 28-year-old male BLM (GM02932) show minor band laddering, indicating that GCI is inherent to Bloom syndrome cells generally and therefore is a potential contributor to the genomic instability that initiates tumor development in these patients. The contrast-enhanced right-hand

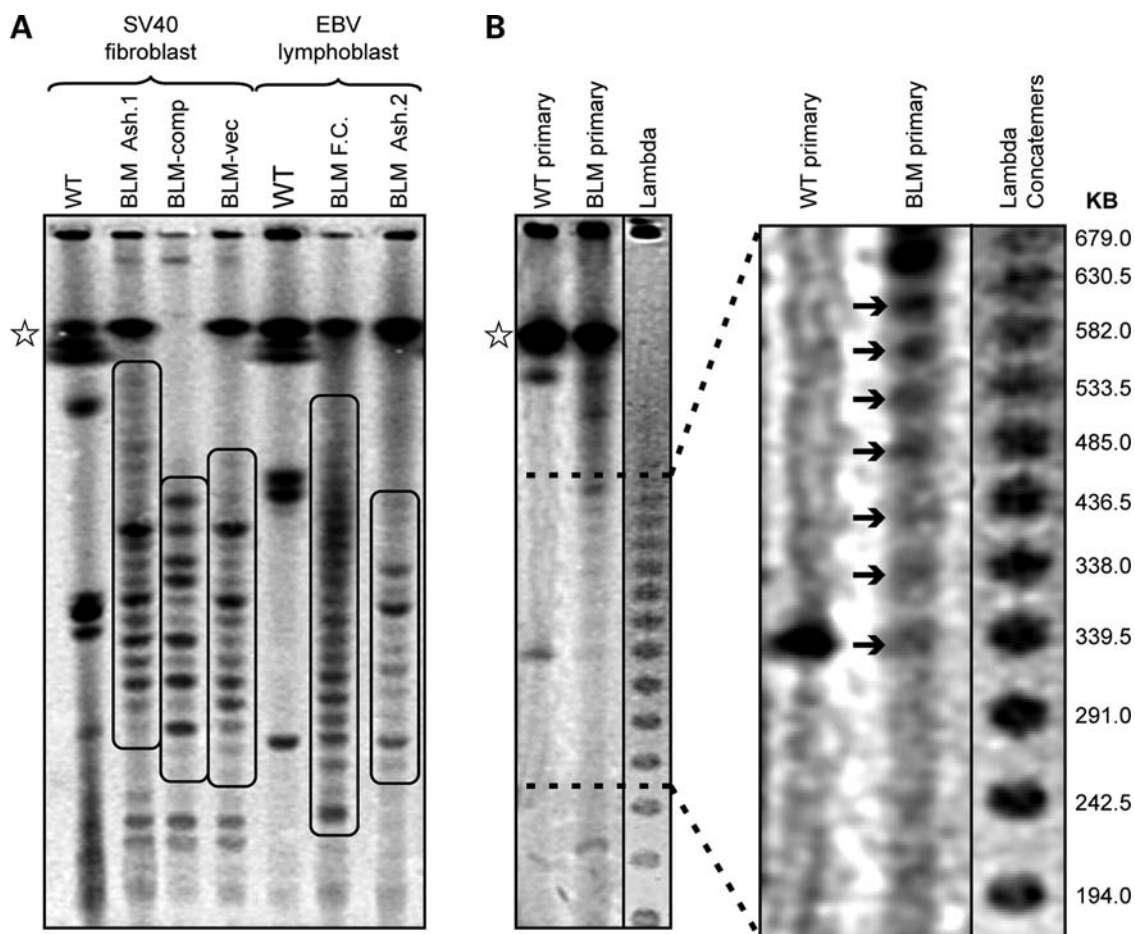


Figure 3. Bloom syndrome GCI. (A) rDNA gene clusters in non-clonal cell line populations resolved to 1 Mb (star). WT: wild-type lines: SV40-transformed (GM00637), EBV-transformed (GM06990). BLM Ash.1: Ashkenazi Jewish, Bloom syndrome registry #42 (GM08505); BLM F.C.: French-Canadian, Bloom syndrome registry #81 (GM16375); BLM Ash.2: Ashkenazi Jewish, Bloom syndrome registry #9 (GM03403); BLM-comp: same as BLM Ash.1 stably complemented with BLM cDNA; BLM-vec: same as BLM Ash.1 stably transfected with empty vector control. Rounded boxes show laddering pattern indicative of a GCI-high phenotype. (B) rDNA gene clusters in primary cells resolved to 1 Mb (star). WT primary: untransformed wild-type fibroblasts (GM01652); BLM primary: untransformed Bloom syndrome fibroblasts, Ashkenazi Jewish, Bloom syndrome registry #3 (GM02932); Lambda: lambda phage concatemers (unit genome size=48 502 bp). Arrows show the minor banding pattern in BLM primary cells in the contrast-enhanced rightmost panel.

panel allows direct comparison of the spacing of the BLM gene cluster laddering with the well-defined length lambda phage concatemers. The BLM ladder (arrows) shows slightly closer spacing than the lambda ladder, consistent with the 43.0 kb rDNA unit gene repeat versus the 48.5 kb lambda genome size.

Complementation of the BLM defect restores rDNA gene cluster stability. Minor band laddering is seen in the bulk populations of two BLM derived lines: BLM-comp and BLM-vec (Fig. 3A). These non-clonal lines are the product of transfection and stable selection of BLM-defective BLM Ash.1 cells with either the pcDNA3 vector expressing full-length wild-type BLM or the pcDNA3 vector alone, respectively (23). Since these are non-clonal lines, the BLM-comp population shows the minor banding pattern of instability that was generated during the BLM-null history of this line. The current stability of the BLM-comp line is revealed by clonal analysis (Fig. 4A). As expected, the minor band laddering in the BLM-comp bulk population resolves as variability in the pattern of major bands in the BLM-comp clonal isolates. The clonal isolates themselves, however, contain a greatly

reduced amount of *de novo* minor banding relative to the BLM-vec non-complemented isogenic line (Fig. 4B), indicating that restoration of the BLM protein has stabilized the rDNA gene clusters.

Since the BLM-comp cells are not completely complemented for the elevated SCE phenotype of Bloom syndrome cells (23) (Supplementary Material) and still show some minor banding indicative of ongoing GCI in the clonal sub-lines (Fig. 4A), we wanted to verify the importance of the BLM protein in promoting gene cluster stability by assaying loss of stability in an otherwise stable line upon loss of the BLM protein. Accordingly, we used shRNA (24) to knockdown expression of BLM in a clonal wild-type GM00637 cell population. We used a 'semi-stable' knockdown technique where the selectable shRNA expression plasmid was transfected and selected for 7 days to kill untransfected cells, followed by dilution plating to single cells and unselected sub-clonal expansion. We used this semi-stable technique to prevent eventual overgrowth by cells losing shRNA expression. After 7 days of selection, BLM levels measured by western

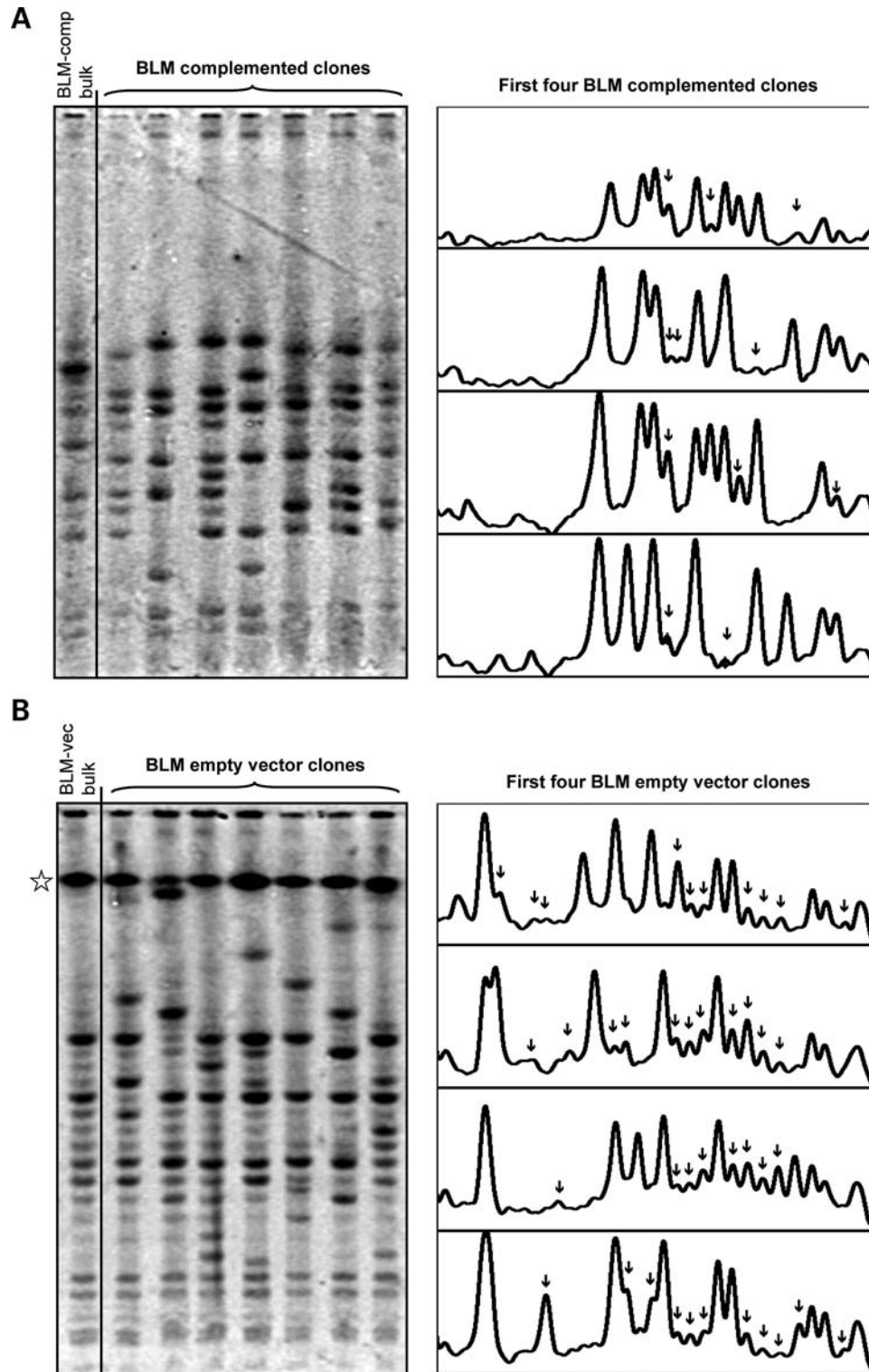


Figure 4. GCI in isogenic BLM and BLM-complemented human cells. (A) BLM-comp bulk population (leftmost lane) and single-cell derived clones resolved to 1 Mb. On the right is a densitometric trace of the first four clonal BLM-comp lines with minor bands indicated by arrows. (B) BLM-vec bulk population (leftmost lane) and single-cell derived clones resolved to 1 Mb (star). On the right is a densitometric trace of the first four clonal BLM-vec lines with minor bands indicated by arrows. Notice the much larger quantity of minor bands observed in the vector-control BLM-defective clonal lines relative to the BLM complemented but otherwise isogenic clonal lines in (A).

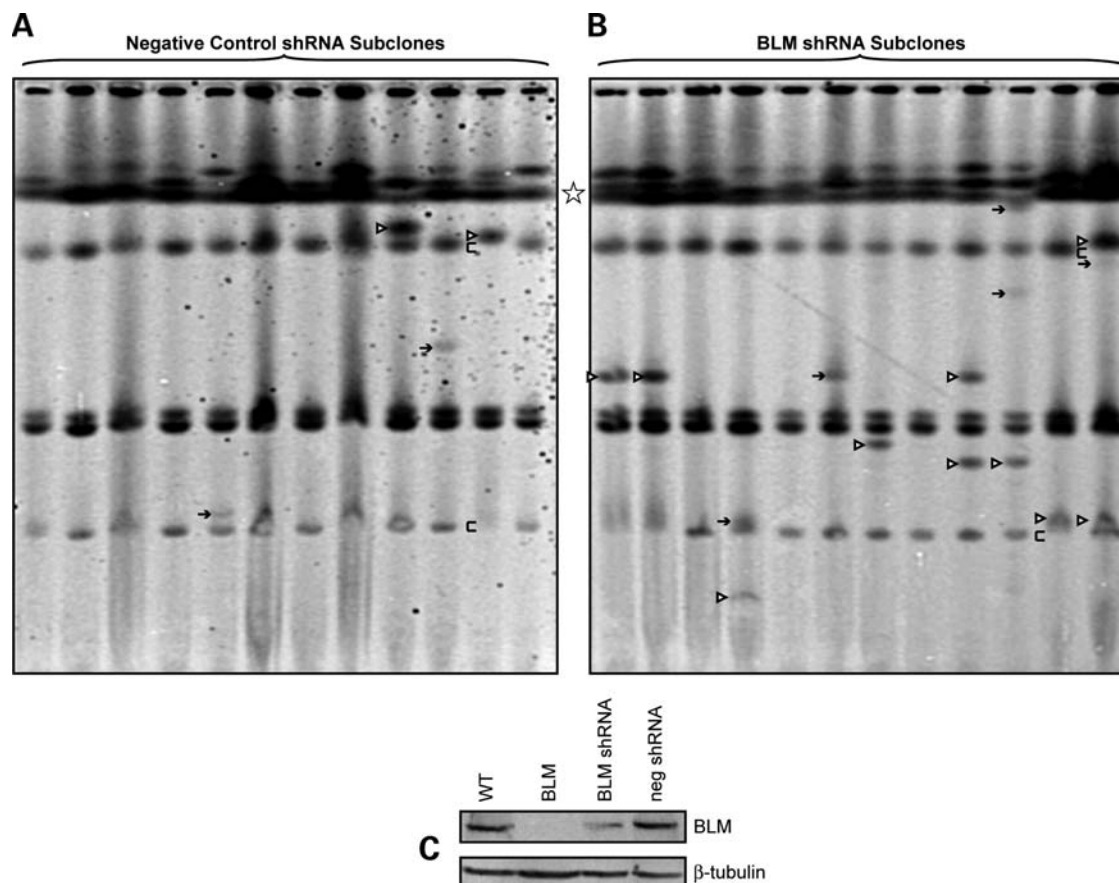


Figure 5. shRNA expressing clonal lines. Gene clusters resolved to 1 Mb (star). Changes to the major banding pattern are shown by open triangles (new bands) and brackets (missing bands). Arrows indicate new minor bands. (A) Sub-clones of a clonal wild-type GM00637 cell population, semi-stably transfected with a negative control shRNA. (B) Sub-clones of the same GM00637 clonal cell population, semi-stably transfected with shRNA to knockdown BLM expression. (C) Western blot showing shRNA knockdown of BLM expression 1 week post-transfection. WT: clonal isolate of wild-type GM00637 cells; BLM: Bloom syndrome GM08505 cells; BLM shRNA: WT cells semi-stably transfected with pCPM-234 (knockdown BLM); neg shRNA: WT cells semi-stably transfected with pCPM-neg (negative control). β -Tubulin is used as a loading control.

blotting were decreased by 70% (Fig. 5C), at which time sub-clonal lines were rederived from single cells. Sub-clonal lines from the clonal cell population transfected with the negative-control shRNA construct pCPM-neg show only limited gene cluster length alterations (Fig. 5A: arrows, brackets and triangles), whereas sub-clonal lines from the same clonal cell population transfected instead with the BLM knockdown shRNA construct pCPM-234 show an approximately 3-fold greater number of gene cluster length alterations (Fig. 5B), again implicating the expression of BLM as a critical stabilizer of these rDNA gene clusters.

Having established a role for BLM in the maintenance of gene cluster genomic integrity, we wanted to determine whether RecQ helicases other than BLM were also involved. We performed clonal GCI analysis on SV40-immortalized fibroblasts from a Werner syndrome patient (Fig. 6) homozygous for a truncating R368X mutation in the WRN gene, a RecQ helicase defective in a strong progeroid syndrome (25). We see no minor bands in a clonal derivative of these WRN-deficient AG11395 cells, and neither changes to the major banding pattern nor new minor bands in single-cell derived sub-clonal populations derived from the clonal cells. We conclude that the suppression of rDNA GCI is not a

property of the RecQ helicase family generally, although we have not yet assayed cells deficient in the remaining RecQ helicases: RECQL, RECQL4 and RECQL5.

An ataxia-telangiectasia mutated cell line has more GCI than HeLa cells. The minor banding we observed in a bulk population of ATM-deficient cells (Fig. 1C) motivated us to use clonal analysis to determine whether there was ongoing GCI in this line. Starting with a clonal isolate each of the apparently gene cluster stable HeLa cells and the apparently gene cluster unstable ATM cells, we generated sub-clonal lines for analysis. In ten sub-clonal HeLa lines (Fig. 7A), we observed one altered major band (triangle) and two new minor bands (arrows) showing the general stability of the HeLa rDNA gene cluster architecture. In contrast, in eight ATM-deficient sub-clones (Fig. 7B), we found one new major band (triangle) and seven newly generated minor bands (arrows), suggesting an elevated rate of GCI in the ATM-deficient line.

We also found that defects in transcription-coupled nucleotide excision repair do not greatly enhance GCI. The Cockayne's syndrome B (CSB) protein ERCC6 required for transcription-coupled nucleotide excision repair (26) has been implicated in the stability of gene clusters with the observation

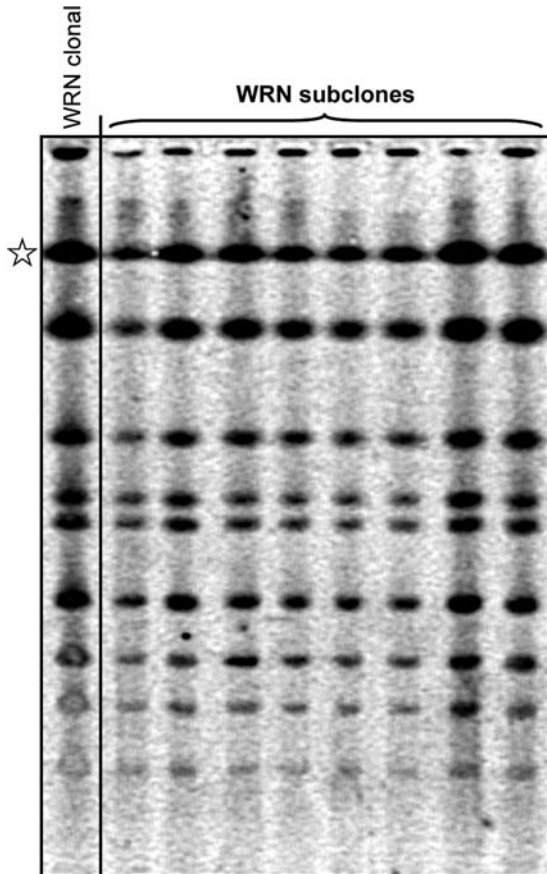


Figure 6. Werner syndrome clonal lines. rDNA gene clusters from WRN-defective SV40-transformed fibroblasts (AG11395) resolved to 1 Mb (star). A clonal population derived from a single cell is shown in the leftmost lane. Sub-clones were derived by dilution plating to single cells with subsequent expansion. No alterations in major gene cluster lengths are observed, and neither are any minor-intensity bands.

that defects in CSB cause aberrant metaphase figures at gene clusters (27). Therefore to ascertain whether a CSB defect obviously compromised stability of the rDNA gene clusters, we generated a clonal population of CSB defective (GM00739) cells. This clonal population 'CSB clonal' exhibited one visible minor band (Fig. 8A, arrow) that is reflected as a major banding pattern gain of this cluster length in four of twelve sub-clones, 'D', 'F', 'H' and 'L' (triangles). Since these four sub-clones also all lose the same major band (bracket), a reasonable interpretation is that around the third mitosis in the expanding 'CSB clonal' population, a spontaneous recombination event in one of the cells caused a gain of two repeats in the cluster indicated by a closed circle to generate the new longer cluster indicated by an arrow. We also observe two additional major band changes (triangles) in sub-clones 'F' and 'H' that do show a corresponding visible minor band in the parental population at the open circle indicators. Evidently, the events that lead to these major banding changes happened late enough in the parental population expansion that the fraction of cells carrying the change is below the limit of detection for a minor band in the 'CSB clonal' population. Nevertheless, the number of minor and major banding alterations in the CSB-defective

cells is not greatly larger than that seen in similar clonal analysis with either HeLa (Fig. 7A) or wild-type SV40-transformed fibroblasts (Fig. 2A), leading us to conclude that the CSB-dependent repair pathway is not significantly involved in rDNA gene cluster stability.

We similarly detect no large increase in instability with loss of the NHEJ pathway. In experiments that quantify double-strand break mediated non-crossover gene conversion, loss of critical NHEJ proteins such as XRCC6, XRCC5, PRKDC (Ku70/80/DNA-PK_{cs}) or XRCC4 cause an increase in recombination of between 3-fold and 5-fold (28). Nevertheless, a non-clonal population of cells derived from a patient with a defect in DNA ligase IV, the obligate heterodimeric partner of XRCC4 (29), appears gene cluster stable, with one clearly defined resolved major band and no apparent minor banding (Fig. 1C). To confirm this apparent stability, we compared rDNA banding patterns in clonal human isogenic NALM-6 cells, and NALM-6 cells in which DNA ligase IV was disrupted by gene targeting (30). In the wild-type NALM-6 cells, we observe one minor band in the non-clonal bulk population (Fig. 8B, arrow) that gave an altered major band in sub-clone 'C' of the three sub-clonal NALM-6 lines, likely the result of loss of one repeat from the gene cluster indicated by the closed circle. We likewise see a major band change in NALM-6 clone 'B' from a late event arising from a small sub-population of the bulk parental line (open circle). In the DNA ligase IV knockout NALM-6 cells, we see one major band alteration in sub-clone 'C', again arising from a small sub-population in the 'LIG4 ko bulk' population. In none of the six clonal lines from either NALM-6 or NALM-6 lines knocked out for DNA ligase IV do we see minor bands, indicating that rapid ongoing recombination-mediated rearrangement of rDNA gene clusters is not occurring, and ruling out DNA ligase IV as a strong player in maintaining rDNA gene cluster stability.

DISCUSSION

The GCI assay is philosophically similar to the microsatellite instability (MSI) assay for defective mismatch repair. In MSI+ lines, polymerase slippage at repetitive mono-, di- and tri-nucleotide short tandem repeats (STRs) generates expansions and contractions of the STR length, which are not subsequently corrected by mismatch repair (reviewed in 31). In contrast, the repeated sequences assayed here for GCI are thousands of base pairs in length, requiring a completely different underlying biochemistry for stability than the microsatellites. We propose that the mechanism causing GCI is dysregulated homologous recombination, where the usual strong bias in favor of short-tract gene conversion without crossing over (32) has been lost or attenuated. The kind of crossover recombination reactions capable of producing the GCI we observe in the BLM-deficient cells is ordinarily highly suppressed.

The known biochemical ability of BLM and partner proteins to dissolve double Holliday junctions, in combination with the ladder-like pattern of instability we describe here, is consistent with a crossover recombination mechanism for gene cluster destabilization in the absence of BLM. Nevertheless,

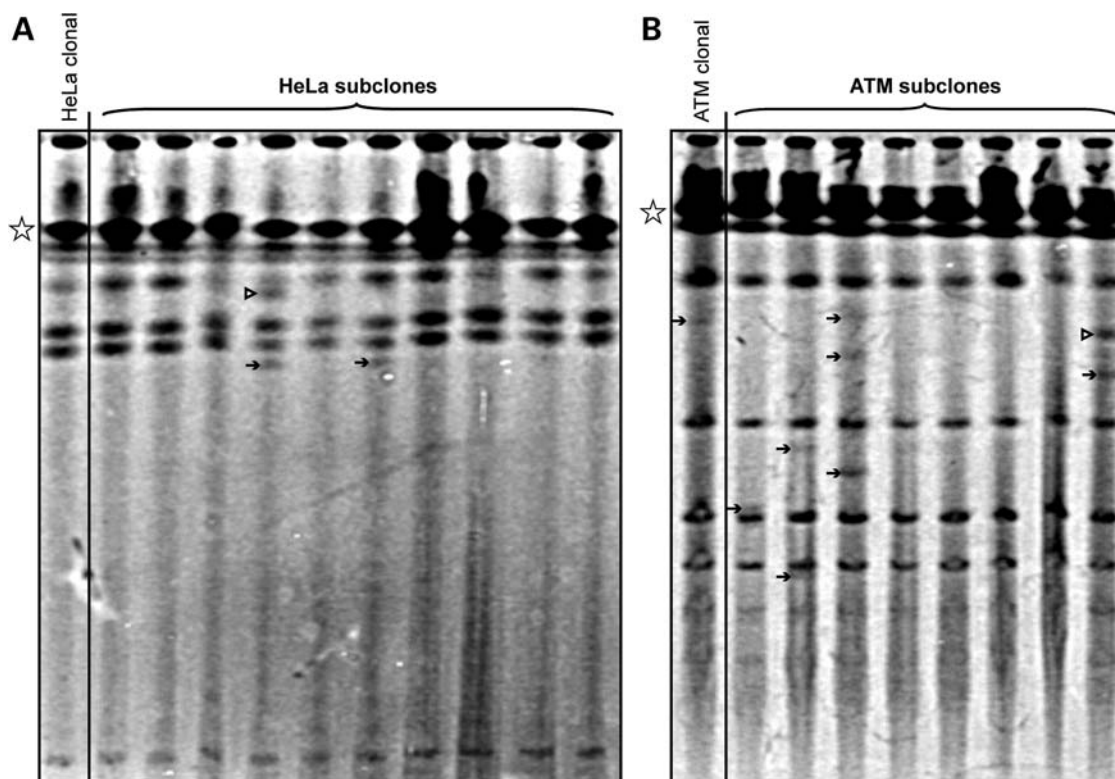


Figure 7. HeLa versus ATM-deficient clonal analysis (A) HeLa cells. (B) ATM deficient cells. Gene clusters are resolved to 1 Mb (star). Changes to major banding patterns are indicated by open triangles. Arrows show new minor bands indicative of rearrangement during clonal expansion.

we cannot rule out the possibility that gene cluster length alteration is a product of break-induced replication (BIR) (reviewed in 33), either in whole or in part. Indeed, a microhomology mediated break-induced replication model has been recently proposed as a mechanism for the generation of many human genomic copy number variations (34).

It is also formally possible that in the absence of BLM, the rDNA gene clusters we assay in this work are being broken and then rejoined by a translocation-like mechanism driven by NHEJ. Since NHEJ does not require alignment of homologous sequences as does recombination, generation of the single repeat 43 kb changes in gene cluster length we observe would additionally require the gene clusters to break at one specifically defined sequence within a unit repeat. Conceivably some kind of BLM-suppressed chromosome fragility structure could produce this kind of sequence-specific breakage pattern, potentially quadruplex-G sequences (35) or hemicatenated replication structures (36). The lack of a significant increase in GCI in the absence of DNA ligase IV, however, argues that if rearrangements are initiated by frank chromosomal breaks, NHEJ is not a competing pathway for these breaks. Accordingly we do not favor the notion of frank double-strand breaks as the primary initiating events in rDNA GCI but prefer the previously suggested idea (28) that recombination can be initiated from one-sided double-strand ends arising from collapsed replication forks. It is attractive to speculate that this putative replication fork collapse is caused by the formation of quadruplex-G sequences in the G/C-rich rDNA, since the BLM protein efficiently unwinds

quadruplex-G DNA (37). It will be interesting to determine whether loss of the BRIP1 (FANCD1) protein, which has a similar ability to unwind quadruplex-G (38), will likewise cause rDNA GCI.

The human BLM protein has been characterized as facilitating the EXO1 mediated 5'-3' resection of double-strand breaks prior to allowing the loading of the RAD51 recombinase (39,40). The highly elevated recombination phenotypes observed in the absence of BLM, however, argue against the requirement for this activity of BLM in either rDNA gene cluster recombination or SCE. Likewise, human BLM also possesses a single-stranded DNA (ssDNA) annealing activity (41,42) that appears uninvolved in these particular recombination processes. In contrast, BLM also possesses an anti-recombinogenic capacity to remove invaded 3' ssDNA tails from D-loops (43,44), including the disruption of a pre-formed RAD51 filament (45). Loss of this BLM activity likely contributes to elevated recombination phenotypes in Bloom syndrome cells.

We assayed the repeated 43 kb genes comprising the rDNA gene clusters in the belief that these clusters were the most likely to show spontaneous recombination-mediated alterations due to their abundance, length, degree of sequence conservation and number of potentially interacting chromosomes. Intriguingly, the size of chromatin loops in HeLa cells has been characterized as averaging 86 kb (46), which is the exact length of two rDNA genes and may be important in the propensity of recombination to alter rDNA gene cluster lengths. Looped chromatin generally may be an important

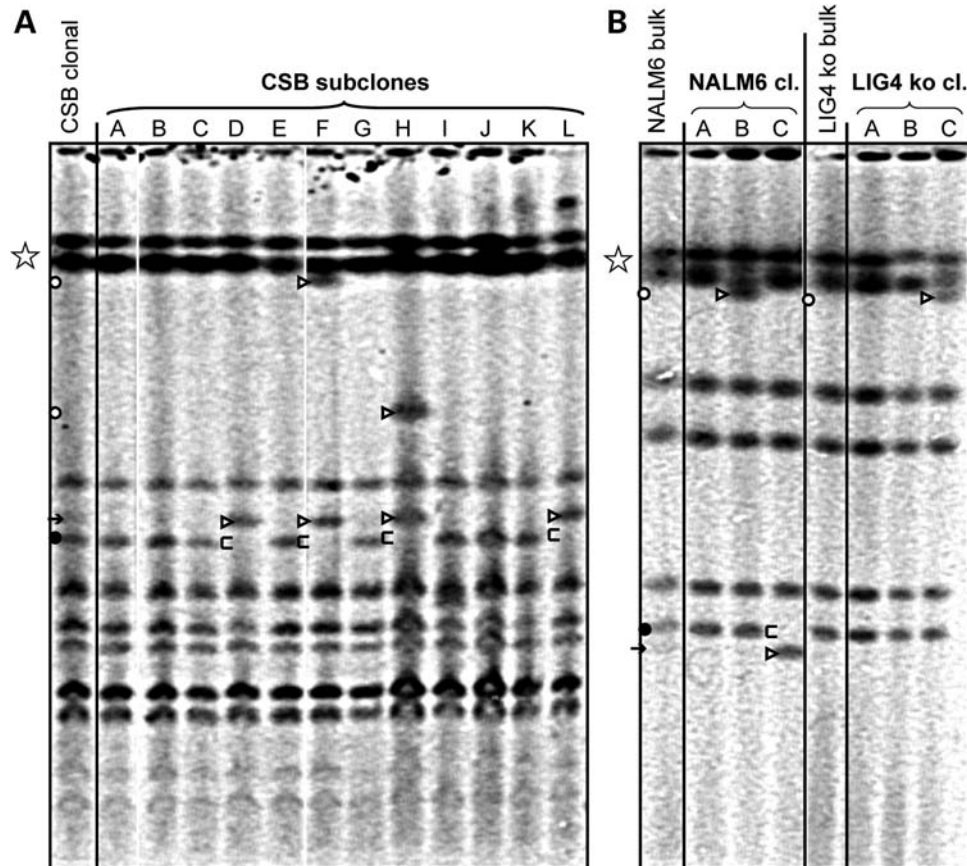


Figure 8. CSB-deficient and wild-type versus DNA-ligase IV knockout cell clonal analysis. (A) CSB-deficient cells. (B) Wild-type NALM-6 cells and NALM-6 cells gene targeted to inactivate DNA ligase IV. Gene clusters are resolved to 1 Mb (star). Changes to major banding patterns are indicated by open triangles. Brackets indicate loss of major bands. Minor bands are shown by arrows. Locations of predicted but unobserved minor bands in parental populations based on new major bands observed in clonally derived sub-populations (triangles) are shown by open circles. The fraction of cells in the parental population carrying clusters of these lengths is below the detection capability of the assay.

intermediate in gene cluster recombination, and the tendency for chromatin loop domains to be long may protect shorter gene clusters from intramolecular recombination. It will be interesting to determine if the spontaneous gene cluster reorganization seen here in the rDNA can also be observed in smaller, less abundant non-rDNA gene clusters (47), although we would predict having fewer potentially recombining gene clusters of shorter overall length would decrease the ability to sensitively detect alterations in other gene cluster loci. Consistent with a role in protecting particularly susceptible classes of gene clusters such as the rDNA from recombination, BLM protein sub-cellular localization includes the nucleolus (48), possibly for the specific purpose of counteracting the potential for recombination to destabilize the rDNA gene clusters that are also located in the nucleolus. Seen in this light, the nucleolus may function specifically as a recombination-suppression sub-nuclear zone. It will also be of interest for future studies to determine whether chemical agents known to induce SCE lead to a parallel increase in GCI, and whether the GCI assay can be a useful measure of sub-microscopic genomic toxicity.

To a first-order approximation, by comparing the number of observed minor bands per clonal isolate, we find the rate of spontaneous alterations in gene cluster architecture to be

over 100-fold elevated in cells lacking BLM (9.6 minor bands per clone) and 10-fold elevated in cells lacking ATM (0.9 minor bands per clone) compared with wild-type controls (0.08 minor bands per clone). It is intriguing that the rDNA GCI we observe in BLM and to a lesser extent in ATM cells parallels the increased cancer predisposition in Bloom syndrome and ataxia-telangiectasia patients. Particularly, because crossover recombination between low-copy human genomic repeats has the potential to generate enormous genomic instability through formation of dicentric and acentric chromosomes, it remains to be seen whether or not GCI, whether caused by functional loss of BLM or otherwise, is a common mechanism of genomic instability driving the etiology and progression of human cancer.

MATERIALS AND METHODS

Cell lines

Cell lines GM00637 (wt), GM09607 (ATM), GM08505 (BLM), GM13136 (FANCC), GM16097 (LIG1), GM16089 (LIG4), GM15989 (NBN), AG11395 (WRN), GM00739 (CSB) were from the Coriell Cell Repository and maintained in minimal essential (MEM) with 10% fetal bovine serum

(FBS). The lines GM06990 (wt), GM01652 (wt), GM02932 (BLM), GM16375 (BLM) and GM03403 (BLM), also from the Coriell Cell Repository, were maintained in either MEM or RPMI media with 15% FBS. BJ-5ta and HeLa S3 cells were from ATCC (CRL-4001 and CCL-2.2, respectively), grown in MEM with 10% FBS. CGM1 cells were from RIKEN, also grown in MEM with 10% FBS. The isogenic cell lines BLM-comp (GM08505 + BLM cDNA, also known as PSNF5) and BLM-vec (GM08505 + vector control, also known as PSNG13) were kindly provided by Hickson (23) and maintained in MEM with 10% FBS with the addition of 0.35 mg/ml G418. NALM-6 DNA ligase IV knockout cells have been previously described (30). All cell lines were grown at 37°C and in 5% CO₂ in a humidified incubator.

DNA isolation and Southern analysis

High molecular weight genomic DNA was isolated from cells in agarose, digested with *EcoRV* to liberate intact rDNA gene clusters, resolved on pulse-field gels with resolution from 10 kb to 1 Mb and probed with radiolabeled rDNA sequences according to methods given by Stults *et al.* (21).

Western blotting

Cells were lysed with RIPA buffer [50 mM Tris-HCl (pH 7.4), 150 mM NaCl 1% NP-40, 1% deoxycholate, 0.1% SDS and 1 mM EDTA] containing a cocktail of protease inhibitors (Pierce, cat. 78410) for 5 min at 4°C. Whole-cell lysates were separated on 8% SDS-polyacrylamide gels, and proteins transferred to a nitrocellulose membrane and subjected to western blotting analysis with rabbit anti-BLM antibody (Calbiochem, cat. DR1034) or rabbit anti- β -tubulin (Thermo, cat. RB-9249-P). The secondary antibody used was HRP-conjugated donkey anti-rabbit IgG (Pierce, cat. 31458). Blots were detected with ECL plus western blotting detection system (Pierce, cat. RPN2132) and visualized on a Storm 860 PhosphorImager (Molecular Dynamics) via chemifluorescence.

Cytogenetics

SCEs were visualized in stained metaphase spreads according to Perry and Wolff (4) with minor modifications.

shRNA

The plasmids pCPM-234 (deplete BLM) and pCPM-neg (negative control) were derived from plasmids V2HS_89234 and RHS1707 (Open Biosystems), respectively. The shRNA sequences were sub-cloned into the 3' untranslated region of a puromycin resistance gene and expressed in a derivative of the pCAGGS vector (49) modified to be incapable of episomal replication. For semi-stable knockdowns, cells were transfected with 10 μ g shRNA plasmids pCPM-234 or pCPM-neg using a BTX ECM 830 square-wave electroporator: nine pulses, 150 V, 7 ms pulse duration, 1 s pulse interval, total volume 750 μ l growth media. Stable integration of the plasmid was selected via puromycin resistance (300 ng/ml) for 1 week, at which time BLM knockdown was measured

by western blotting followed by limited dilution sub-cloning and expansion.

SUPPLEMENTARY MATERIAL

Supplementary Material is available at *HMG* online.

Conflict of Interest statement. None declared.

FUNDING

This work was supported by the Kentucky Lung Cancer Research Program.

REFERENCES

- German, J. (1997) Bloom's syndrome. XX. The first 100 cancers. *Cancer Genet. Cytogenet.*, **93**, 100–106.
- Chaganti, R.S., Schonberg, S. and German, J. (1974) A manyfold increase in sister chromatid exchanges in Bloom's syndrome lymphocytes. *Proc. Natl Acad. Sci. USA*, **71**, 4508–4512.
- German, J., Archibald, R. and Bloom, D. (1965) Chromosomal breakage in a rare and probably genetically determined syndrome of man. *Science*, **148**, 506–507.
- Perry, P. and Wolff, S. (1974) New Giemsa method for the differential staining of sister chromatids. *Nature*, **251**, 156–158.
- Ellis, N.A., Groden, J., Ye, T.Z., Straughen, J., Lennon, D.J., Ciocci, S., Proytcheva, M. and German, J. (1995) The Bloom's syndrome gene product is homologous to RecQ helicases. *Cell*, **83**, 655–666.
- Bohr, V.A. (2008) Rising from the RecQ-age: the role of human RecQ helicases in genome maintenance. *Trends Biochem. Sci.*, **33**, 609–620.
- Raynard, S., Zhao, W., Bussen, W., Lu, L., Ding, Y.Y., Busygina, V., Meetei, A.R. and Sung, P. (2008) Functional role of BLAP75 in BLM-topoisomerase IIIalpha-dependent Holliday junction processing. *J. Biol. Chem.*, **283**, 15701–15708.
- Xu, D., Guo, R., Sobeck, A., Bachrati, C.Z., Yang, J., Enomoto, T., Brown, G.W., Hoatlin, M.E., Hickson, I.D. and Wang, W. (2008) RMI, a new OB-fold complex essential for Bloom syndrome protein to maintain genome stability. *Genes Dev.*, **22**, 2843–2855.
- Raynard, S., Bussen, W. and Sung, P. (2006) A double Holliday junction dissolution complex comprising BLM, topoisomerase IIIalpha, and BLAP75. *J. Biol. Chem.*, **281**, 13861–13864.
- Wu, L., Bachrati, C.Z., Ou, J., Xu, C., Yin, J., Chang, M., Wang, W., Li, L., Brown, G.W. and Hickson, I.D. (2006) BLAP75/RMI1 promotes the BLM-dependent dissolution of homologous recombination intermediates. *Proc. Natl Acad. Sci. USA*, **103**, 4068–4073.
- Ip, S.C., Rass, U., Blanco, M.G., Flynn, H.R., Skehel, J.M. and West, S.C. (2008) Identification of Holliday junction resolvases from humans and yeast. *Nature*, **456**, 357–361.
- Consortium, I.H.G.S. (2004) Finishing the euchromatic sequence of the human genome. *Nature*, **431**, 931–945.
- Gu, W., Zhang, F. and Lupski, J.R. (2008) Mechanisms for human genomic rearrangements. *Pathogenetics*, **1**, 4.
- Kyoizumi, S., Nakamura, N., Takebe, H., Tatsumi, K., German, J. and Akiyama, M. (1989) Frequency of variant erythrocytes at the glycoprotein-A locus in two Bloom's syndrome patients. *Mutat. Res.*, **214**, 215–222.
- Langlois, R.G., Bigbee, W.L., Jensen, R.H. and German, J. (1989) Evidence for increased *in vivo* mutation and somatic recombination in Bloom's syndrome. *Proc. Natl Acad. Sci. USA*, **86**, 670–674.
- Ellis, N.A., Lennon, D.J., Proytcheva, M., Alhadef, B., Henderson, E.E. and German, J. (1995) Somatic intragenic recombination within the mutated locus BLM can correct the high sister-chromatid exchange phenotype of Bloom syndrome cells. *Am. J. Hum. Genet.*, **57**, 1019–1027.
- Groden, J., Nakamura, Y. and German, J. (1990) Molecular evidence that homologous recombination occurs in proliferating human somatic cells. *Proc. Natl Acad. Sci. USA*, **87**, 4315–4319.
- Groden, J. and German, J. (1992) Bloom's syndrome. XVIII. Hypermutability at a tandem-repeat locus. *Hum. Genet.*, **90**, 360–367.

19. Gonzalez, I.L. and Sylvester, J.E. (1995) Complete sequence of the 43-kb human ribosomal DNA repeat: analysis of the intergenic spacer. *Genomics*, **27**, 320–328.
20. Henderson, A.S., Warburton, D. and Atwood, K.C. (1972) Location of ribosomal DNA in the human chromosome complement. *Proc. Natl Acad. Sci. USA*, **69**, 3394–3398.
21. Stults, D.M., Killen, M.W., Pierce, H.H. and Pierce, A.J. (2008) Genomic architecture and inheritance of human ribosomal RNA gene clusters. *Genome Res.*, **18**, 13–18.
22. Luria, S.E. and Delbruck, M. (1943) Mutations of bacteria from virus sensitivity to virus resistance. *Genetics*, **28**, 491–511.
23. Gaymes, T.J., North, P.S., Brady, N., Hickson, I.D., Mufti, G.J. and Rassool, F.V. (2002) Increased error-prone non homologous DNA end-joining—a proposed mechanism of chromosomal instability in Bloom's syndrome. *Oncogene*, **21**, 2525–2533.
24. Stegmeier, F., Hu, G., Rickles, R.J., Hannon, G.J. and Elledge, S.J. (2005) A lentiviral microRNA-based system for single-copy polymerase II-regulated RNA interference in mammalian cells. *Proc. Natl Acad. Sci. USA*, **102**, 13212–13217.
25. Yu, C.E., Oshima, J., Fu, Y.H., Wijisman, E.M., Hisama, F., Alisch, R., Matthews, S., Nakura, J., Miki, T., Ouais, S. *et al.* (1996) Positional cloning of the Werner's syndrome gene. *Science*, **272**, 258–262.
26. Hanawalt, P.C. and Spivak, G. (2008) Transcription-coupled DNA repair: two decades of progress and surprises. *Nat. Rev. Mol. Cell Biol.*, **9**, 958–970.
27. Yu, A., Fan, H.Y., Liao, D., Bailey, A.D. and Weiner, A.M. (2000) Activation of p53 or loss of the Cockayne syndrome group B repair protein causes metaphase fragility of human U1, U2 and 5S genes. *Mol. Cell*, **5**, 801–810.
28. Pierce, A.J., Hu, P., Han, M., Ellis, N. and Jasin, M. (2001) Ku DNA end-binding protein modulates homologous repair of double-strand breaks in mammalian cells. *Genes Dev.*, **15**, 3237–3242.
29. Wu, P.Y., Frit, P., Meesala, S., Dauvillier, S., Modesti, M., Andres, S.N., Huang, Y., Sekiguchi, J., Calsou, P., Salles, B. *et al.* (2009) Structural and functional interaction between the human DNA repair proteins DNA Ligase IV and XRCC4. *Mol. Cell Biol.*, **29**, 3163–3172.
30. Iizumi, S., Nomura, Y., So, S., Uegaki, K., Aoki, K., Shibahara, K., Adachi, N. and Koyama, H. (2006) Simple one-week method to construct gene-targeting vectors: application to production of human knockout cell lines. *Biotechniques*, **41**, 311–316.
31. Laghi, L., Bianchi, P. and Malesci, A. (2008) Differences and evolution of the methods for the assessment of microsatellite instability. *Oncogene*, **27**, 6313–6321.
32. Paques, F., Leung, W.Y. and Haber, J.E. (1998) Expansions and contractions in a tandem repeat induced by double-strand break repair. *Mol. Cell Biol.*, **18**, 2045–2054.
33. Llorente, B., Smith, C.E. and Symington, L.S. (2008) Break-induced replication: what is it and what is it for? *Cell Cycle*, **7**, 859–864.
34. Hastings, P.J., Ira, G. and Lupski, J.R. (2009) A microhomology-mediated break-induced replication model for the origin of human copy number variation. *PLoS Genet.*, **5**, e1000327.
35. Huber, M.D., Duquette, M.L., Shiels, J.C. and Maizels, N. (2006) A conserved G4 DNA binding domain in RecQ family helicases. *J. Mol. Biol.*, **358**, 1071–1080.
36. Fricke, W.M. and Brill, S.J. (2003) Slx1–Slx4 is a second structure-specific endonuclease functionally redundant with Sgs1-Top3. *Genes Dev.*, **17**, 1768–1778.
37. Sun, H., Karow, J.K., Hickson, I.D. and Maizels, N. (1998) The Bloom's syndrome helicase unwinds G4 DNA. *J. Biol. Chem.*, **273**, 27587–27592.
38. London, T.B., Barber, L.J., Mosedale, G., Kelly, G.P., Balasubramanian, S., Hickson, I.D., Boulton, S.J. and Hiom, K. (2008) FANCD1 is a structure-specific DNA helicase associated with the maintenance of genomic G/C tracts. *J. Biol. Chem.*, **283**, 36132–36139.
39. Gravel, S., Chapman, J.R., Magill, C. and Jackson, S.P. (2008) DNA helicases Sgs1 and BLM promote DNA double-strand break resection. *Genes Dev.*, **22**, 2767–2772.
40. Nimonkar, A.V., Ozsoy, A.Z., Genschel, J., Modrich, P. and Kowalczykowski, S.C. (2008) Human exonuclease 1 and BLM helicase interact to resect DNA and initiate DNA repair. *Proc. Natl Acad. Sci. USA*, **105**, 16906–16911.
41. Cheok, C.F., Wu, L., Garcia, P.L., Janscak, P. and Hickson, I.D. (2005) The Bloom's syndrome helicase promotes the annealing of complementary single-stranded DNA. *Nucleic Acids Res.*, **33**, 3932–3941.
42. Machwe, A., Xiao, L., Groden, J., Matson, S.W. and Orren, D.K. (2005) RecQ family members combine strand pairing and unwinding activities to catalyze strand exchange. *J. Biol. Chem.*, **280**, 23397–23407.
43. Bachrati, C.Z., Borts, R.H. and Hickson, I.D. (2006) Mobile D-loops are a preferred substrate for the Bloom's syndrome helicase. *Nucleic Acids Res.*, **34**, 2269–2279.
44. van Brabant, A.J., Ye, T., Sanz, M., German, I.J., Ellis, N.A. and Holloman, W.K. (2000) Binding and melting of D-loops by the Bloom syndrome helicase. *Biochemistry (Mosc.)*, **39**, 14617–14625.
45. Bugreev, D.V., Yu, X., Egelman, E.H. and Mazin, A.V. (2007) Novel pro- and anti-recombination activities of the Bloom's syndrome helicase. *Genes Dev.*, **21**, 3085–3094.
46. Jackson, D.A., Dickinson, P. and Cook, P.R. (1990) The size of chromatin loops in HeLa cells. *EMBO J.*, **9**, 567–571.
47. Warburton, P.E., Hasson, D., Guillem, F., Lescale, C., Jin, X. and Abrusan, G. (2008) Analysis of the largest tandemly repeated DNA families in the human genome. *BMC Genomics*, **9**, 533.
48. Sanz, M.M., Proytcheva, M., Ellis, N.A., Holloman, W.K. and German, J. (2000) BLM, the Bloom's syndrome protein, varies during the cell cycle in its amount, distribution, and co-localization with other nuclear proteins. *Cytogenet. Cell Genet.*, **91**, 217–223.
49. Niwa, H., Yamamura, K. and Miyazaki, J. (1991) Efficient selection for high-expression transfectants with a novel eukaryotic vector. *Gene*, **108**, 193–199.